Musilova, M., Tranter, M., Wadham, J., Telling, J., Tedstone, A., & Anesio, A. (2017). Microbially-driven export of labile organic carbon from the Greenland Ice Sheet. *Nature Geoscience*, *10*(5), 360–365. https://doi.org/10.1038/ngeo2920

Peer reviewed version

Microbially-driven export of labile organic carbon from the Greenland Ice Sheet

Michaela Musilova[1]*, Martyn Tranter[1], Jemma Wadham[1], Jon Telling[1], Andrew Tedstone[2] and Alexandre M. Anesio[1]**

[1] Bristol Glaciology Centre, School of Geographical Sciences, University of Bristol, Bristol, UK

[2] School of Geoscience, University of Edinburgh, Edinburgh, UK

* Present address:
Slovak Organisation for Space Activities (SOSA), Bratislava, Slovakia
& Faculty of Electrical Engineering and Information Technology of the Slovak University of Technology, Bratislava, Slovakia

** Present address:
Bristol Glaciology Centre, School of Geographical Sciences, University of Bristol, Bristol, UK

Abstract

Glaciers and ice sheets are significant sources of dissolved organic carbon and nutrients to downstream subglacial and marine ecosystems. Climatically-driven increases in glacial runoff are expected to intensify the impact of exported nutrients on local and regional downstream environments. However, the origin and bioreactivity of dissolved organic carbon from glacier surfaces are not fully understood. Here, we present data comprising of simultaneous measurements of gross primary production, community respiration, dissolved organic carbon composition and export from different surface habitats of the Greenland Ice Sheet, throughout the ablation season. We found that microbial production was significantly correlated with the concentration of labile dissolved organic species in glacier surface meltwater (Pearson correlation $p<0.001$). Further, we determined that freely-available organic compounds made up 62% of the dissolved organic carbon exported from the glacier surface through streams. We therefore conclude that microbial communities were the primary driver for labile dissolved organic carbon production and recycling on glacier surfaces (up to 1.12 ± 0.14 mg C $L^{-1}d^{-1}$ carbon production), and that glacier dissolved organic carbon export is dependent on active microbial processes during the melt season.

43 The Greenland Ice Sheet (GrIS) is the second largest body of ice on Earth, after the Antarctic
44 Ice Sheet, covering ~1.71x10^6 km^2 [1]. The GrIS has ~350 ocean-terminating outlets[2] and an
45 annual meltwater runoff of ~400 km^3, comparable to the average annual discharge from a
46 large Arctic river, such as the Ob[3, 4, 5]. Recent studies have found glacial runoff to be a
47 significant source of highly bioavailable nutrients to downstream ecosystems[3, 6, 7, 8]. In
48 particular, glacial meltwater exports labile dissolved organic carbon (DOC), which is rich in
49 protein-like low molecular weight compounds (LMWC) and distinct from non-glacially
50 derived riverine DOC[3, 8], which has a high proportion of aromatic and higher molecular
51 weight compounds[9]. High glacial meltwater fluxes, therefore, have an important impact on
52 downstream marine heterotrophic and primary productivity on local[10] and regional scales[11].

53 The origin and nature of the glacial dissolved organic matter (DOM) is still a subject of
54 debate. In the Gulf of Alaska, labile DOM exported by glacier runoff from 11 coastal
55 watersheds has an ancient (~4x10^3 year) ^{14}C age signature[7]. Stubbins *et al.* (2012)[12] have
56 suggested that anthropogenic combustion products are the source of the ancient organic
57 carbon to glacier surfaces, which account for the ^{14}C-depletion observed by Hood *et al.*
58 (2009)[7]. On the other hand, Singer *et al.* (2012)[13] found that combustion products only
59 marginally contribute to the DOM from Alpine glaciers and that the DOM is more likely
60 derived from *in situ* microbial activity. So far, there have been very few studies on the origin
61 of the GrIS DOC, even though the GrIS runoff has been substantially increasing since 1992 at
62 a rate of 16.9 ± 1.8 km^3 yr^{-1} [5]. The climatically driven changes in GrIS meltwater fluxes[14]
63 could thus dramatically increase the quantity of reactive glacial DOC exported to the coastal
64 waters surrounding Greenland[3, 7, 15].

65 Previous work has concentrated on the discharge of DOC from glacial termini, with only
66 limited complementary water sampling and studies of supraglacial (glacier surface) microbial
67 processes on the GrIS.[3, 8, 16]. The supraglacial DOC measured to date had a terrestrial $\delta^{13}C$

signature and was rich in nitrogen[16]. Conversely, the subglacial DOC contained allochthonous-derived carbon both from soils and vegetation, as well as carbon derived from microbial processes[3, 16]. The limited data suggested that autochthonous microbial activity accounted for the majority of the supraglacial DOC. Lawson *et al.* (2014)[8] also studied DOC concentrations in glacial runoff from an outlet glacier at the southwestern margin of the GrIS, with a focus on the quality, quantity and temporal variation of DOC fluxes over two contrasting melt seasons. They postulated that the physicochemical and microbiological cycling of carbon at the glacier surface is a major source of the bioavailable DOC, complemented by biogeochemical processes at the ice sheet bed[8, 17].

Autotrophic microbial communities at the glacier surface are believed to fix atmospheric carbon and thereby generate bioavailable autochthonous DOC (including LMWC) through photosynthesis, while heterotrophic processes consume and recycle this labile DOC[16, 18, 19, 20]. The balance between net production and consumption varies between sampling sites on the GrIS[18, 21, 22, 23, 24]. The highest microbial activity is commonly concentrated in glacier surface debris (cryoconite)[18, 25, 26]. Enhanced melting of the ice surface around the dark-coloured cryoconite leads to the formation of small (0.01-1 m in diameter and 0.01-0.5 m deep) water-filled, debris-based depressions, called 'cryoconite holes'[27, 28, 29]. Cryoconite and cryoconite hole waters host abundant viruses, prokaryotes and eukaryotes responsible for the biogeochemical cycling of carbon and other nutrients [30, 31, 32]. Bare ice and snow also contains a wide variety of microorganisms, including algae[33], which may fix substantially more CO_2 than cryoconite holes because of the greater spatial extent of this habitat[24, 34].

However, the link between supraglacial autochthonous microbial DOC production and GrIS DOC export has only been postulated until now. To date, no study has analysed the inputs and transformations of the DOC in parallel with the microbial net ecosystem production (NEP) on the GrIS surface, throughout a complete ablation season. NEP is defined as the

93 difference between gross photosynthetic (GP) organic carbon (C) production and
94 consumption through respiration (R) in an ecosystem, where NEP = GP - R[35]. Furthermore,
95 previous studies have not assessed the evolution of the microbial activity over an entire
96 summer melt season and how it impacts on the characteristics of exported DOC. Here, for the
97 first time, the changes in DOC species and concentrations were analysed in different GrIS
98 supraglacial habitats (snow, clean ice, cryoconite debris and cryoconite holes) in association
99 with measurements of GP and R. We determined the: 1) external sources of C added to
100 supraglacial ecosystems; 2) consumption and production of new C by local microbial
101 communities; and 3) the nature of the DOC that was exported from the glacier through
102 supraglacial streams to downstream environments, during an entire melt season.
103
104 Sampling was conducted on Leverett Glacier (~67.10ºN, 50.20ºW) in the southwest of the
105 GrIS. The sampling site was a delimited circular area 8 m in diameter, chosen randomly ~2
106 km from the terminus of the glacier. Dispersed cryoconite debris on the glacier surface ('dirty
107 ice'), clean ice, stream water, cryoconite hole water ('cryowater') and cryoconite hole
108 sediment were sampled once every 10-14 days, during the 2012 ablation season, between 15th
109 May and 1st August. Ice cores were collected during the first two sampling time points in
110 order to analyse the contents of the ice frozen over winter, which was released as meltwater
111 later in the season. Waters were collected from supraglacial streams flowing away from the
112 sampling site into a nearby moulin, which supplies the drainage system beneath the glacier
113 and the river emerging from Leverett Glacier[36]. Snow samples were collected on May 13th,
114 before snowmelt had occurred and thus the snowpack had minimal to no meltwaters
115 disturbing it. The surface snow turned to slush by 15th May, before melting away by 20th
116 May. The collected samples were divided into three different sample types: principal sources
117 of meltwater (snow and ice – studied through the ice cores), supraglacial habitats (dirty ice,

clean ice, cryowater and cryoconite hole sediment) and exported meltwater (stream). GP and R was determined for all of the supraglacial habitats throughout the melt season. Fluorescence spectroscopy and measurements of the concentration of DOC and LMWC (free carbohydrates, amino acids and volatile fatty acids (VFA)) were performed on all samples (see Methods).

Highly active and net autotrophic ecosystems

All four habitat types studied were active and net autotrophic ecosystems, producing significantly more organic C through GP than that being consumed by R. These data are presented as GP = NEP + R in Figure 1a and R in Figure 1b for all the incubations. There were significant differences in C production between the habitat types throughout the season (2-way ANOVA, $p<0.001$). The highest photosynthetic activity in all sample types was at the beginning of the ablation season (0.35-1.12 mg C $L^{-1}d^{-1}$ of C production), equal to 0.28-0.82 mg C $L^{-1}d^{-1}$ of NEP (GP - R). This was followed by a sharp decrease in GP rates until the rates stabilised around 0.06-0.27 mg C $L^{-1}d^{-1}$ of C production (0.03-0.18 mg C $L^{-1}d^{-1}$ of NEP) in June and July, before increasing slightly at the end of the summer. NEP, GP and R rates measured at this site ~2 km from the GrIS margin were comparable to the rates measured over the same summer 35 km from the GrIS margin[24]. Previous NEP measurements on the GrIS have been of short duration only, providing 'snap-shots' of the microbial activities at a certain time, and therefore missed the varying trends in NEP over the ablation season.

All averaged synchronous fluorescence spectra of the supraglacial samples (where λ emission = λ excitation + 18 nm) exhibited the same dominant fluorescence emission peaks (~337,

409-420, 465-479 and ~523 nm), but with varying intensities (Figure 2). The averaged fluorescence spectra for all of the samples were normalised to the fluorescence peak spectral maximum, by dividing the intensity of the emissions measured by the maximum emission intensity that was measured in the entire dataset, to qualitatively assess the proportions of the proteinaceous-like and humic-like fluorophores in the DOC[8, 37, 38]. Fluorescence emission peaks at ~337 nm are indicative of protein-like fluorophores (e.g. tryptophan)[39], and peaks in the range of 409-420, 465-479 and ~523 nm are likely associated with humic and fulvic acid compounds[39, 40, 41]. The snow samples exhibited the lowest normalised spectral fluorescence, together with the ice cores (, apart from the large peak at 337 nm). By contrast, cryowater had an extremely strong peak at 409-420 nm, which was significantly greater than the normalised fluorescence intensity of the other samples at that wavelength. The similarity between the dirty ice and stream spectra is noteworthy, while the average normalized clean ice fluorescence intensity was in between the stream and snow spectra. Additionally, the clean ice, dirty ice and stream samples had a peak at 575 nm, unlike the other samples. This peak is often associated with the algal photosynthetic pigment phycoerithin[8, 42]. Similar compounds have been detected previously in supraglacial meltwaters, snow and cryowater[8, 16]. The presence of fulvic and humic acids, protein-like fluorophores and an algal pigment substantiate our hypothesis that the DOC in all sample types is mostly microbially-derived from photosynthetic algae and bacterial communities[16, 43, 44]. Microbial modification of the autochthonous-derived supraglacial DOC and allochthonous OC into additional bioavailable compounds, through bacterial decomposition, is potentially the source of the significant amounts of humic acids in the cryoconite holes[28, 45]. It is also possible that the fulvic and humic acids in cryoconites holes could be derived from allochthonous inputs of higher plant material[16, 43, 44].

Significant modification of supraglacial labile organic carbon

There were also significant differences in DOC concentrations between the sample types over the whole season (2-way ANOVA, $p<0.001$) (Figure 3). The dirty and clean ice had the highest concentrations of DOC at the start of the season (up to 0.32±0.02 mg C L^{-1}), before decreasing to 0.18±0.02 mg C L^{-1} by the end of the melt season. Cryowater DOC remained at a fairly constant concentration of 0.15±0.01 mg C L^{-1}, which was mirrored in the cryowater GP rates remaining steady throughout the ablation season as well. Stream DOC concentrations started off very low in mid-May (0.09±0.01 mg C L^{-1}). They then peaked in mid-July 2012 (0.23±0.04 mg C L^{-1}), before decreasing again at the end of the summer. The decline in surface ice DOC concentrations was most likely a result of the decreasing GP activity over the melt season (Figure 1) and continuous heterotrophic consumption. Conversely, the ice cores collected at the beginning of the season had much lower DOC concentrations (0.14±0.02 mg C L^{-1}) than the dirty/clean ice samples, and the snow samples had the lowest DOC concentrations (0.06±0.01 mg C L^{-1}). This is in agreement with the hypothesis that NEP throughout the melt season produces the DOC. Moreover, continuous ice melt over the ablation season also led to fresh glacier surfaces being uncovered (not colonised by microbes), thereby diluting the exported DOC. The drop in dirty/clean ice productivity could also be indicative of a limitation in vital nutrients for microbial activity, such as nitrogen and phosphorous in the surface ice, although some recycling potentially stimulated new microbial production towards the end of the season.

The total LMWC concentrations for all of the supraglacial habitats, over the whole ablation season, accounted for ~59% of the average DOC concentrations for these habitats (Table 1). In contrast, only ~41% of the average DOC in snow and ice core samples was made up of

193 LMWC. Overall, ~62% of the DOC exported from the glacier surface, via the studied stream,
194 contained bioavailable LMWC. The variations in LMWC concentrations for all sample types,
195 throughout the 2012 ablation season, are displayed in Figure 4. Carbohydrates had the highest
196 LMWC concentrations (up to 190.9±24.0 μg C L^{-1}), while the amino acids and VFA
197 concentrations only peaked at 67.5±8.4 and 20.6±2.5 μg C L^{-1}, respectively. There were
198 significant differences between the carbohydrate concentrations of the snow and ice core
199 samples, and those of the supraglacial habitats (2-way ANOVA, $p<0.01$). Amino acid
200 concentrations for all sample types peaked in June 2012. The averaged seasonal individual
201 free amino acid, carbohydrate and VFA concentrations, for all sample types, are shown in
202 Supplementary Information Tables 1-3. These concentrations are consistent with previously
203 reported DOC and LMWC in supraglacial samples[3, 8, 16]. The high concentrations of
204 bioavailable LMWC observed here (e.g. glucose, galactose and tyrosine) could be associated
205 with recent microbial photosynthetic activity and biosynthesis[45, 46, 47].
206
207 Both the DOC and LMWC concentrations in dirty/clean ice samples were higher than those
208 in the principal sources of meltwater (one-way ANOVA; $p<0.001$ and $p<0.01$, respectively)
209 at the beginning of the season. For example, DOC in ice cores and snow only contributed to
210 approximately one third of the surface DOC concentrations (Figure 3). There were significant
211 correlations between the total LMWC and DOC concentrations (Pearson correlation's R^2 =
212 0.48, $p<0.001$) and the total free carbohydrate and DOC concentrations (Pearson correlation's
213 $R^2 = 0.46$, $p<0.001$), for the clean/dirty ice, ice core and snow samples (Figure 5). Our results
214 therefore show that supraglacial DOC is made up of significant amounts of labile LMWC,
215 which vary in concentrations and individual compound content over the summer season.
216 However, there was no positive correlation between the LMWC and DOC for the cryowater
217 samples. The cryowater DOC thus likely contains greater amounts of higher molecular

weight compounds, such as humic and fulvic acids. This is in agreement with spectrofluorescence data (Figure 2), indicating great amounts of humic and fulvic type compounds in cryowater than in the other samples. Consequently, microbial processes in clean/dirty ice appear to be primarily responsible for the net production of labile DOC, particularly at the start of the season, while microbial communities in cryoconite holes have a greater importance in modifying and decomposing organic matter from both autochthonous and allochthonous origin. It is highly likely that the DOC and LMWC, remaining in the supraglacial environments at the end of the ablation season (Figure 3-4), freeze into the surface ice over winter and are then released the following ablation season through ice melt. We hypothesize, therefore, that even the DOC and LMWC measured in the ice cores likely originated from the microbial DOC produced during previous seasons. Hence, the supraglacial C source was primarily autochthonous and not derived from external allochthonous sources, such as recent snowfall.

Microbially-driven supraglacial DOC export

Microbial GP C production in all of the supraglacial habitats was significantly correlated with labile LMWC and free carbohydrate concentrations (Pearson correlation's $R^2 = 0.49$, $p<0.001$; and $R^2 = 0.59$, $p<0.001$, respectively), throughout the 2012 ablation season (Figure 5). There were also significant correlations, for dirty and clean ice samples, between the LMWC concentrations and GP C production ($R^2 = 0.30$, $p<0.05$ and $R^2 = 0.69$, $p<0.001$, respectively) and carbohydrate concentrations and GP C production ($R^2 = 0.48$, $p<0.001$and $R^2 = 0.64$, $p<0.001$, respectively). In cryowater, there was a significant correlation between the carbohydrate concentrations and GP C production ($R^2 = 0.23$, $p<0.05$), but not between LMWC concentrations and GP C. It is thus likely that the non-carbohydrate fraction of

LMWC (e.g. amino acids and VFA) are due to the microbial modification and decomposition of organic matter in cryoconite holes, with potentially some additional allochthonous inputs, as hypothesized above.

Our results suggest that most of the bioavailable supraglacial DOC is a result of *in situ* microbial GP activity. All of the supraglacial habitats on the margin of the GrIS were net autotrophic ecosystems, producing substantially more C through GP than what was consumed by R throughout the whole melt season (Figure 1). They were thus the most important source of supraglacial DOC, based on the significant correlations between the GP C production, DOC, LMWC and free carbohydrate concentrations examined previously. We also infer that heterotrophic microbial communities were actively modifying the DOC by consuming and decomposing both autochthonous and allochthonous C, particularly in cryoconite holes. Therefore, the high and continuous levels of microbial DOC production and recycling, on the GrIS surface in 2012, demonstrate that glacier surfaces are not just passive receivers and exporters of ancient labile carbon to downstream ecosystems[7]. Furthermore, these ecosystems were very active and dynamic over the course of one the ablation season, leading to varying amounts and types of DOC exported from the GrIS surface to downstream environments (Figures 3-4). The export of DOC to the moulin peaked in mid-July 2012, before decreasing again at the end of the summer. On average, the DOC exported by the supraglacial stream contained a concentration of microbially-derived fluorophores most similar to that of dirty ice habitats (Figure 2) and ~62% bioavailable LMWC (Table 1). The substantial microbial contribution to DOC production and transformation must, therefore, be included in future estimates of climate change driven DOC export from the GrIS and its effects on the downstream ecosystems.

References

1. Easterbrook DJ, Ollier CD, Carter RM. Observations: The Cryosphere. *Climate Change Reconsidered II* 2013**:** 629-712.

2. Lewis SM, Smith LC. Hydrologic drainage of the Greenland Ice Sheet. *Hydrol Process* 2009, **23:** 2004-2011.

3. Bhatia MP, Das SB, Xu L, Charette MA, Wadham JL, Kujawinski EB. Organic carbon export from the Greenland ice sheet. *Geochim Cosmochim Ac* 2013, **109:** 329-344.

4. Dittmar T, Kattner G. The biogeochemistry of the river and shelf ecosystem of the Arctic Ocean: a review. *Mar Chem* 2003, **83:** 103-120.

5. Bamber J, van den Broeke M, Ettema J, Lenaerts J, Rignot E. Recent large increases in freshwater fluxes from Greenland into the North Atlantic. *Geophys Res Lett* 2012, **39:** L19501.

6. Bhatia MP, Kujawinski EB, Das SB, Breier CF, Henderson PB, Charette MA. Greenland meltwater as a significant and potentially bioavailable source of iron to the ocean. *Nat Geosci* 2013, **6:** 274-278.

7. Hood E, Fellman J, Spencer RGM, Hernes PJ, Edwards R, D'Amore D*, et al.* Glaciers as a source of ancient and labile organic matter to the marine environment. *Nature* 2009, **462:** 1044-U1100.

8. Lawson EC, Wadham JL, Tranter M, Stibal M, Lis GP, Butler CEH*, et al.* Greenland Ice Sheet exports labile organic carbon to the Arctic oceans. *Biogeosciences* 2014, **11:** 4015-4028.

9. Repeta DJ, Quan TM, Aluwihare LI, Accardi A. Chemical characterization of high molecular weight dissolved organic matter in fresh and marine waters. *Geochim Cosmochim Ac* 2002, **66:** 955-962.

10. Rysgaard S, Vang T, Stjernholm M, Rasmussen B, Windelin A, Kiilsholm S. Physical conditions, carbon transport, and climate change impacts in a northeast Greenland fjord. *Arct Antarct Alp Res* 2003, **35:** 301-312.

11. Statham PJ, Skidmore M, Tranter M. Inputs of glacially derived dissolved and colloidal iron to the coastal ocean and implications for primary productivity. *Global Biogeochem Cy* 2008, **22:** Gb3013.

12. Stubbins A, Hood E, Raymond PA, Aiken GR, Sleighter RL, Hernes PJ*, et al.* Anthropogenic aerosols as a source of ancient dissolved organic matter in glaciers. *Nat Geosci* 2012, **5:** 198-201.

13. Singer GA, Fasching C, Wilhelm L, Niggemann J, Steier P, Dittmar T, *et al.* Biogeochemically diverse organic matter in Alpine glaciers and its downstream fate. *Nat Geosci* 2012, **5:** 710-714.

14. Hanna E, Huybrechts P, Steffen K, Cappelen J, Huff R, Shuman C, *et al.* Increased runoff from melt from the Greenland Ice Sheet: A response to global warming. *J Climate* 2008, **21:** 331-341.

15. Hood E, Battin TJ, Fellman J, O'Neel S, Spencer RGM. Storage and release of organic carbon from glaciers and ice sheets. *Nature Geosci* 2015, **8:** 91-96.

16. Bhatia MP, Das SB, Longnecker K, Charette MA, Kujawinski EB. Molecular characterization of dissolved organic matter associated with the Greenland ice sheet. *Geochim Cosmochim Ac* 2010, **74:** 3768-3784.

17. Lawson EC, Bhatia MP, Wadham JL, Kujawinski EB. Continuous Summer Export of Nitrogen-Rich Organic Matter from the Greenland Ice Sheet Inferred by Ultrahigh Resolution Mass Spectrometry. *Environ Sci Technol* 2014, **48:** 14248-14257.

18. Anesio AM, Hodson AJ, Fritz A, Psenner R, Sattler B. High microbial activity on glaciers: importance to the global carbon cycle. *Global Change Biol* 2009, **15:** 955-960.

19. Anesio AM, Sattler B, Foreman C, Telling J, Hodson A, Tranter M*, et al.* Carbon fluxes through bacterial communities on glacier surfaces. *Ann Glaciol* 2010, **51:** 32-40.

20. Hodson A, Anesio AM, Ng F, Watson R, Quirk J, Irvine-Fynn T*, et al.* A glacier respires: Quantifying the distribution and respiration CO2 flux of cryoconite across an entire Arctic supraglacial ecosystem. *Journal of Geophysical Research: Biogeosciences* 2007, **112:** G04S36.

21. Hodson A, Boggild C, Hanna E, Huybrechts P, Langford H, Cameron K*, et al.* The cryoconite ecosystem on the Greenland ice sheet. *Ann Glaciol* 2010, **51:** 123-129.

22. Stibal M, Telling J, Cook J, Mak KM, Hodson A, Anesio AM. Environmental Controls on Microbial Abundance and Activity on the Greenland Ice Sheet: A Multivariate Analysis Approach. *Microb Ecol* 2012, **63:** 74-84.

23. Cook JM, Hodson AJ, Anesio AM, Hanna E, Yallop M, Stibal M*, et al.* An improved estimate of microbially mediated carbon fluxes from the Greenland ice sheet. *J Glaciol* 2012, **58:** 1098-1108.

24. Chandler DM, Alcock JD, Wadham JL, Mackie SL, Telling J. Seasonal changes of ice surface characteristics and productivity in the ablation zone of the Greenland Ice Sheet. *The Cryosphere Discuss* 2014, **8:** 1337-1382.

25. Tranter M, Fountain AG, Fritsen CH, Lyons WB, Priscu JC, Statham PJ*, et al.* Extreme hydrochemical conditions in natural microcosms entombed within Antarctic ice. *Hydrol Process* 2004, **18:** 379-387.

26. Hodson AJ, Mumford PN, Kohler J, Wynn PM. The High Arctic glacial ecosystem: new insights from nutrient budgets. *Biogeochemistry* 2005, **72:** 233-256.

27. Gerdel RW, Drouet F. The cryoconite of the Thule Area, Greenland. *Trans Am Microsc Soc* 1960, **79:** 256–272.

28. Takeuchi N, Kohshima S, Seko K. Structure, formation, and darkening process of albedo-reducing material (cryoconite) on a Himalayan glacier: A granular algal mat growing on the glacier. *Arct Antarct Alp Res* 2001, **33:** 115-122.

29. Fountain AG, Tranter M, Nylen TH, Lewis KJ, Mueller DR. Evolution of cryoconite holes and their contribution to meltwater runoff from glaciers in the McMurdo Dry Valleys, Antarctica. *J Glaciol* 2004, **50:** 35-45.

30. Sawstrom C, Mumford P, Marshall W, Hodson A, Laybourn-Parry J. The microbial communities and primary productivity of cryoconite holes in an Arctic glacier (Svalbard 79 degrees N). *Polar Biol* 2002, **25:** 591-596.

31. Anesio AM, Mindl B, Laybourn-Parry J, Hodson AJ, Sattler B. Viral dynamics in cryoconite holes on a high Arctic glacier (Svalbard). *Journal of Geophysical Research: Biogeosciences* 2007, **112:** G04S31.

32. Edwards A, Anesio AM, Rassner SM, Sattler B, Hubbard B, Perkins WT*, et al.* Possible interactions between bacterial diversity, microbial activity and supraglacial hydrology of cryoconite holes in Svalbard. *Isme J* 2011, **5:** 150-160.

33. Cameron KA, Hagedorn B, Dieser M, Christner BC, Choquette K, Sletten R*, et al.* Diversity and potential sources of microbiota associated with snow on western portions of the Greenland Ice Sheet. *Environ Microbiol* 2015, **17:** 594-609.

34. Yallop ML, Anesio AM, Perkins RG, Cook J, Telling J, Fagan D*, et al.* Photophysiology and albedo-changing potential of the ice algal community on the surface of the Greenland ice sheet. *Isme J* 2012, **6:** 2302-2313.

35. Lovett GM, Cole JJ, Pace ML. Is Net Ecosystem Production Equal to Ecosystem Carbon Accumulation? *Ecosystems* 2006, **9:** 152-155.

36. Chandler DM, Wadham JL, Lis GP, Cowton T, Sole A, Bartholomew I*, et al.* Evolution of the subglacial drainage system beneath the Greenland Ice Sheet revealed by tracers. *Nat Geosci* 2013, **6:** 195-198.

37. Chen J, LeBoef EJ, Dai S, Gu BH. Fluorescence spectroscopic studies of natural organic matter fractions. *Chemosphere* 2003, **50:** 639-647.

38. Baker A, Lamont-Black J. Fluorescence of dissolved organic matter as a natural tracer of ground water. *Ground Water* 2001, **39:** 745-750.

39. Hudson N, Baker A, Reynolds D. Fluorescence analysis of dissolved organic matter in natural, waste and polluted waters - A review. *River Res Appl* 2007, **23:** 631-649.

40. Miano TM, Senesi N. Synchronous Excitation Fluorescence Spectroscopy Applied to Soil Humic Substances Chemistry. *Sci Total Environ* 1992, **118:** 41-51.

41. Ferrari GM, Mingazzini M. Synchronous Fluorescence-Spectra of Dissolved Organic-Matter (Dom) of Algal Origin in Marine Coastal Waters. *Mar Ecol Prog Ser* 1995, **125:** 305-315.

42. Lombardi AT, Jardim WF. Fluorescence spectroscopy of high performance liquid chromatography fractionated marine and terrestrial organic materials. *Water Res* 1999, **33:** 512-520.

43. Lafreniere MJ, Sharp MJ. The concentration and fluorescence of dissolved organic carbon (DOC) in glacial and nonglacial catchments: Interpreting hydrological flow routing and DOC sources. *Arct Antarct Alp Res* 2004, **36:** 156-165.

44. Barker JD, Sharp MJ, Fitzsimons SJ, Turner RJ. Abundance and dynamics of dissolved organic carbon in glacier systems. *Arct Antarct Alp Res* 2006, **38:** 163-172.

45. Barker JD, Sharp MJ, Turner RJ. Using synchronous fluorescence spectroscopy and principal components analysis to monitor dissolved organic matter dynamics in a glacier system. *Hydrol Process* 2009, **23:** 1487-1500.

46. Biersmith A, Benner R. Carbohydrates in phytoplankton and freshly produced dissolved organic matter. *Mar Chem* 1998, **63:** 131-144.

47. Kirchman DL, Meon B, Ducklow HW, Carlson CA, Hansell DA, Steward GF. Glucose fluxes and concentrations of dissolved combined neutral sugars (polysaccharides) in the Ross Sea and Polar Front Zone, Antarctica. *Deep-Sea Res Pt Ii* 2001, **48:** 4179-4197.

Acknowledgements

This study was funded by grants from the UK National Environment Research Council (NERC) NE/J02399X/1 to Anesio, NERC Doctoral Training Program Grant to Musilova, NERC grant NE/H023879/1 to Wadham and NERC studentships NE/152830X/1 and NE/J500021/1 to Tedstone. We would like to thank all members of the Greenland 2012 Leverett field team for their assistance during field work.

Author Contributions:

M.M., A.M.A and J.T. designed the overall study. M.T. and J.W. were involved in advising the detail of the study design. M.M. and A.T. collected the field data. M.M. performed the experiment and processed the data. M.M., A.M.A. and M.T. wrote the paper. All authors discussed the results and commented on the manuscript.

Corresponding author:

Dr. Michaela Musilova

email: michaela.musilova@community.isunet.edu

Competing financial interests

The authors declare that they have no competing financial interests.

Figure legends:

Figure 1. Gross photosynthesis [GP; net ecosystem production (NEP) + respiration (R)] and R variability over one ablation season is shown in panels a and b, respectively, in the different supraglacial habitats. GP and R rates are expressed in mg C $L^{-1}d^{-1}$ as C produced through photosynthesis and C consumed through R, respectively. All of the habitats sampled were net autotrophic ecosystems, producing more C from CO_2 through photosynthesis than what was being consumed through respiration. Standard errors were calculated as 1σ with n = 3.

475 **Figure 2.** Averaged synchronous fluorescence spectra collected over the entire summer 2012
476 for the studied glacier surface sample types (where **λ** emission = **λ** excitation + 18 nm). All
477 averaged spectra have been normalised to the fluorescence peak spectral maximum, by
478 dividing the intensity of the emissions measured by the maximum emission intensity that was
479 measured in the entire dataset, to assess the proportions of fluorophores in dissolved organic
480 carbon. The same dominant fluorescence emission peaks (at ~337, 409-420, 465-479 and
481 ~523 nm excitation) were present in all sample types.

482

483 **Figure 3.** Variations in 2012 ablation season DOC concentrations in supraglacial samples (in
484 mg C L^{-1}). There were significant differences in DOC concentrations between the sample
485 types over the season (2-way ANOVA, $p<0.001$). All sample types exhibited a decline in
486 DOC at the end of the season, except for cryowater. Cryowater DOC remained fairly
487 constantly at 0.15±0.01 mg C L^{-1} throughout the ablation season. Snow and ice core samples
488 were collected at the beginning of the ablation season to estimate the addition of DOC from
489 external sources to the supraglacial environments. Standard errors were calculated as 1σ (n =
490 6).

491

492 **Figure 4.** Variations in supraglacial low molecular weight compound concentrations
493 (LMWC) of total free: a) amino acids, b) carbohydrates and c) volatile fatty acids (VFA) for
494 all sample types, per sampling time point, throughout the 2012 ablation season. Standard
495 errors were calculated as 1σ with n = 84, n = 54 and n = 30, respectively.

496

497 **Figure 5.** Total LMWC (a) and free carbohydrates (b) were compared vs. DOC, throughout
498 the 2012 ablation season, for: all supraglacial habitat samples n = 21 (7 averaged samples

each of cryowater, dirty ice and clean ice (where n=3 per sample type, per time point), n = 2 for the ice cores and n = 1 for the snow). Total LMWC (c) and free carbohydrates (d) were compared vs. GP C production, throughout the 2012 ablation season, for: cryowater, dirty ice, and clean ice (n = 63, where there are 21 samples of cryowater, dirty ice and clean ice each).

Table 1. Total LMWC concentrations for all of the different sample types, averaged over the whole 2012 ablation season. The LMWC component of the average DOC is indicated for the supraglacial habitats (dirty ice, clean ice and cryowater), principal sources of meltwater (snow and ice – studied through ice cores) and for the DOC exported through the studied stream. Detailed data for each individual LMWC is provided in the Supplementary Information Tables 1-3. Standard errors were calculated as 1σ with n = 3528, n = 2268 and n = 1260, for amino acids, carbohydrates and VFA, respectively.

LMWC	Total LMWC concentration for all sample types (μgCL^{-1})	Total LMWC component of supraglacial habitat DOC (%)	Total LMWC component of meltwater DOC (%)	Total LMWC component of exported DOC (%)
amino acids	37.81 ± 4.25	19.03 ± 0.02	21.06 ± 0.05	21.87 ± 0.03
carbohydrates	61.58 ± 10.14	33.16 ± 0.45	12.37 ± 1.04	32.40 ± 0.59
VFA	13.54 ± 1.77	6.81 ± 0.01	7.90 ± 0.02	7.78 ± 0.02
Sum of all LMWC	112.93 ± 11.14	59.00 ± 0.45	41.33 ± 1.03	62.05 ± 0.59

Methods

520

521 **Field sampling strategy**

522 All sample types were collected aseptically into sterile Whirl-Pak bags (Nasco) during the
523 2012 ablation season (15th May, 28th May, 11th June, 25th June, 9th July, 23rd July and 1st
524 August). Cryoconite hole, snow and clean/dirty ice sampling, within the delimited sampling
525 site, is described in detail in Musilova *et al.* (2015)[48]. The dirty ice had sediment particle
526 sizes <1 mm and was present in patches within the sampling area[48], while the clean ice did
527 not have any visible sediment particles on nor within the ice. Seventy cm deep ice cores were
528 drilled using a Kovacs ice corer (cleaned by drilling three non-sample cores, since
529 sterilisation for molecular level studies was not necessary) and collected in sterile 5 L Whirl-
530 Pak bags (Nasco). They were drilled in the same location over both the first and consecutive
531 second sampling time points, in order to analyse the meltwater released through surface ice
532 melting down to ~140 cm. Cryowater and stream water was collected using sterile 50 mL
533 syringes (Fisher) into pre-cleaned (rinsed 6x with sterile Milli-Q water (18.2 MΩ cm^{-1}
534 deionized water, filtered through 0.22 μm membranes)) and pre-furnaced (550ºC for 4 hours)
535 borosilicate glass bottles, prior to transport. All samples were transported to the field camp
536 laboratory for processing <2 hrs after collection. Snow and ice samples were melted at
537 ambient temperature (~10ºC) upon transportation to the field camp laboratory. All samples
538 were filtered immediately through a pre-cleaned and pre-furnaced glass filtration apparatus
539 into pre-furnaced borosilicate amber glass bottles. Pre-furnaced 0.70 μm GF/F (Millipore)
540 filters were used for DOC analyses and inline (0.45 μm; Millipore) filters were used for
541 LMWC analyses. Filtrates for DOC analyses were acidified to pH 2-3 with concentrated HCl
542 and stored at ≤4°C in the field laboratory, during transport and storage at the University of
543 Bristol. The other samples were frozen at ≤-20°C in the field freezer, during transport (in
544 insulated containers) and storage at the University of Bristol prior to laboratory analyses, as

had been performed successfully previously Lawson *et al.* (2014)[8]. Triplicate procedural blanks were carried out by collecting autoclaved Milli-Q water into the same containers/Whirl-Pak bags as the samples, filtering it and storing it using the same procedure as applied for the samples.

NEP measurements

NEP is defined as the difference between gross photosynthetic (GP) organic carbon (C) production and consumption through respiration (R) in an ecosystem, where NEP = GP - R[35]. It was determined by incubating six glass bottles per sample, filled with the different supraglacial sample types (cryowater, cryoconite hole sediment, dirty and clean ice) for 24±1 h within cryoconite holes in *in situ* conditions, following previously described methods[24, 49]. Three out of the six bottles were wrapped in foil to prevent light from entering the bottles (in order to only measure respiration), while the other three remained unwrapped to allow for photosynthesis, as well as respiration (to measure NEP)[23]. For the cryoconite hole samples, the debris thickness in the bottles was representative of that in the holes (~1-4 mm thick) and bottles were filled with water collected from the same holes as the debris[24, 49]. The ice samples were melted before pouring into the bottles, as per Chandler et al. (2014)[24]. Changes between the start and end dissolved O_2 concentrations and temperatures in the incubation bottles were measured immediately, after the incubations had finished on the surface of the glacier, using a PreSens Fibox3 fibreoptic O_2 meter with a type PSt1 TS sensor (manufacturer's stated accuracy: ±1%). These measurements were normalized for the different dry weights of the sediment in the bottles, determined by drying and weighing the sediment, then converted to mg C L^{-1} d^{-1} using a programme for temperature-compensated oxygen calculation for PreSens oxygen microsensors (Huber, C., 6.2.2003 – personal

570 communication) and following previously described methods[24, 49]. Altogether, seven different
571 incubation experiments were performed at regular intervals throughout the 2012 GrIS
572 ablation season.
573
574
575 **DOC analyses**
576
577 DOC concentrations were measured in all sample types as non-purgeable organic carbon by
578 high temperature combustion (680°C), using a Shimadzu TOC-VCSN/TNM-1 Analyser
579 equipped with a high sensitivity catalyst, following the methods described by Lawson *et al.*
580 (2014)[8]. The precision, accuracy and limit of detection of the method were <7%, <8% and 30
581 μg C L^{-1}, determined as per Lawson *et al.* (2014)[8].
582
583 **LMWC concentrations**
584
585 Free carbohydrate, amino acid and VFA determinations were performed by an ICS-3000
586 dual-analysis Reagent-Free Ion Chromatography system (Dionex, Sunnyvale, USA),
587 equipped with Chromeleon 6.8 software. Nine carbohydrate fractions (fucose, rhamnose,
588 arabinose, galactose, glucose, xylose/mannose, fructose/sucrose, ribose and lactose) were
589 separated isocratically on a CarboPac PA20 column (3×150 mm), after passing through a
590 CarboPac PA20 guard column (3x30 mm), following previously described methods[8, 50].
591 Fructose/sucrose and xylose/mannose were reported together, due to the carbohydrates co-
592 eluting[8]. Fourteen different free amino acids (lysine, alanine, threonine, glycine, valine,
593 serine, proline, isoleucine, leucine, methionine, phenylalanine, cysteine, aspartic acid,
594 glutamic acid and tyrosine) were separated on an AminoPac PA10 column (2×250 mm), after

passing through an AminoPac PA10 guard column (2x50 mm)[8]. Five VFA (acetate, propionate, formate, butyrate and oxalate) were separated isocratically on an IonPac AS11-HC capillary IC column (2×250 mm), after passing through an IonPac AG11-HC guard column (2x50 mm). Precision was ≤10% and accuracy was < ±9% for all analytes, determined as per Lawson *et al.* (2014)[8].

Fluorescence Spectroscopy

Synchronous fluorescence spectroscopy was performed on a HORIBA Jobin Yvon Fluorolog-3 spectrofluorometer to qualitatively assess the proportions of proteinaceous-like and humic-like fluorophores in the fulvic acid fraction of DOC[8, 37, 38]. The parameters for scanning and post-scanning corrections (Ramen and Rayleigh scattering, and inner-filter effects) were based on previously described protocols, where **λ** emission = **λ** excitation + 18 nm [8, 44, 45]. The fluorescence spectra for all of the samples were normalised to the fluorescence peak spectral maximum (i.e. the maximum fluorescent intensity in all of the samples), by dividing the intensity of the emissions measured by the maximum emission intensity that was measured in the entire dataset, following previously described methods[8, 44, 45].

Data availability

The authors declare that the data supporting the findings of this study are available within the article and its supplementary information files. Further datasets generated during and/or analysed during the current study are available from the corresponding author on reasonable request.

Methods References

48. Musilova M, Tranter M, Bennett SA, Wadham J, Anesio AM. Stable microbial community composition on the Greenland Ice Sheet. *Front Microbiol* 2015, **6:** 193.

49. Telling J, Anesio AM, Hawkings J, Tranter M, Wadham JL, Hodson AJ*, et al.* Measuring rates of gross photosynthesis and net community production in cryoconite holes: a comparison of field methods. *Ann Glaciol* 2010, **51:** 153-162.

50. Stibal M, Lawson EC, Lis GP, Mak KM, Wadham JL, Anesio AM. Organic matter content and quality in supraglacial debris across the ablation zone of the Greenland ice sheet. *Ann Glaciol* 2010, **51:** 1-8.

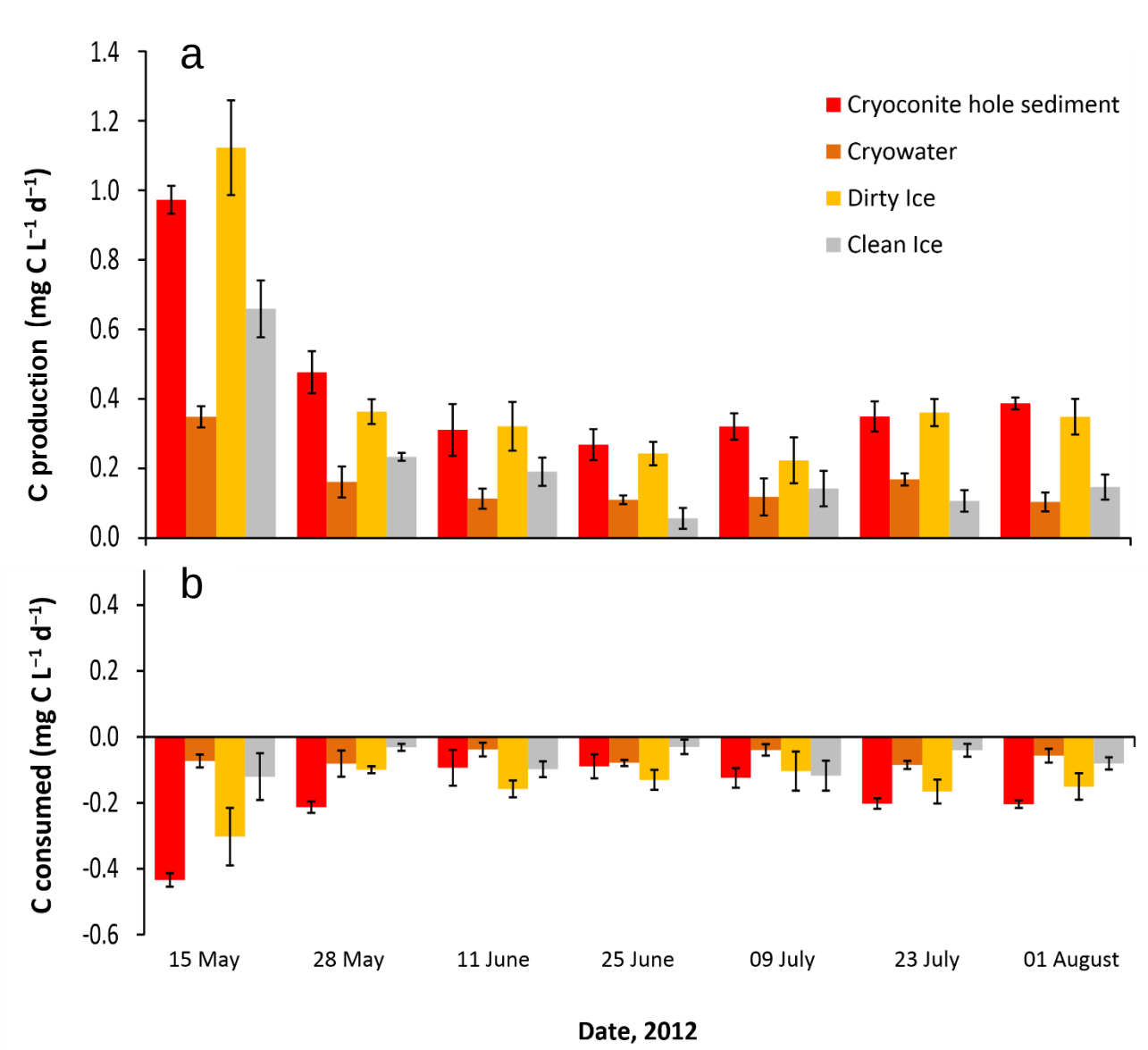
a
b
Cryoconite hole sediment
Cryowater
Dirty Ice
Clean Ice
C production (mg C L-1 d-1)
C consumed (mg C L-1 d-1)
1.4
1.2
1.0
0.8
0.6
0.4
0.2
0.0
-0.2
-0.4
-0.6
15 May
28 May
11 June
25 June
09 July
23 July
01 August
Date, 2012

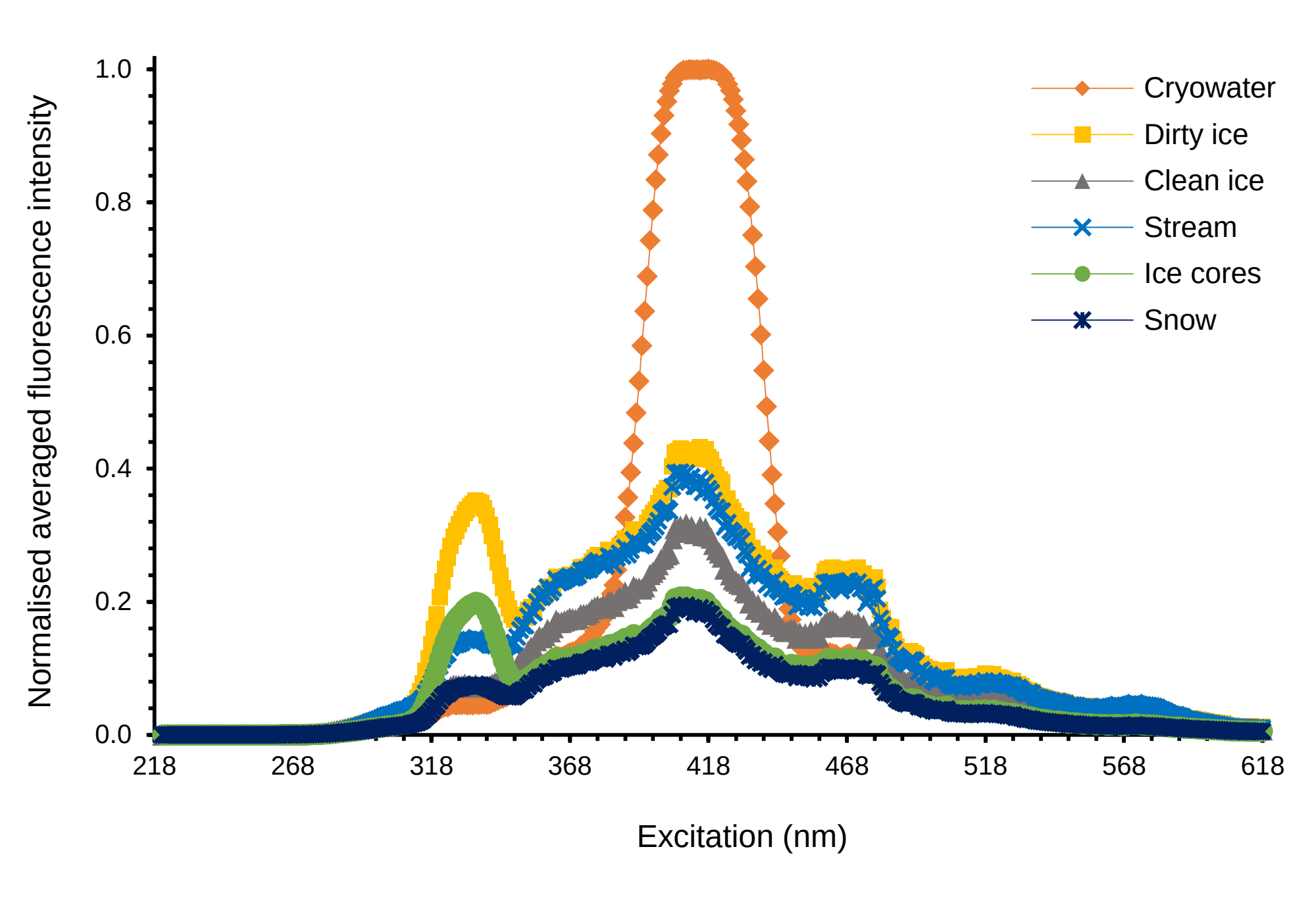
Normalised averaged fluorescence intensity
1.0
0.8
0.6
0.4
0.2
0.0
218
268
318
368
418
468
518
568
618
Excitation (nm)
Cryowater
Dirty ice
Clean ice
Stream
Ice cores
Snow

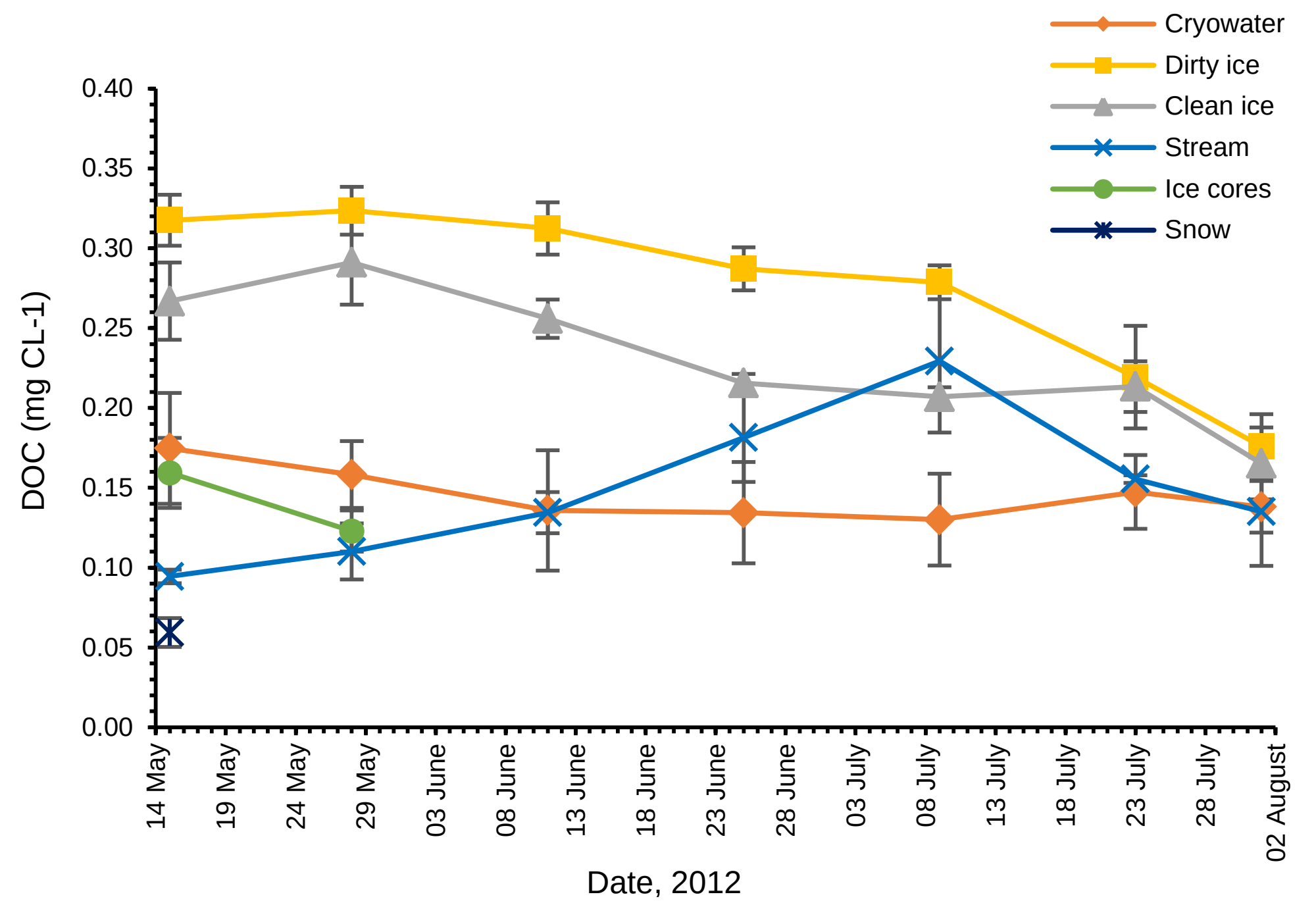
Cryowater
Dirty ice
Clean ice
Stream
Ice cores
Snow
DOC (mg CL-1)
0.40
0.35
0.30
0.25
0.20
0.15
0.10
0.05
0.00
14 May
19 May
24 May
29 May
03 June
08 June
13 June
18 June
23 June
28 June
03 July
08 July
13 July
18 July
23 July
28 July
02 August
Date, 2012

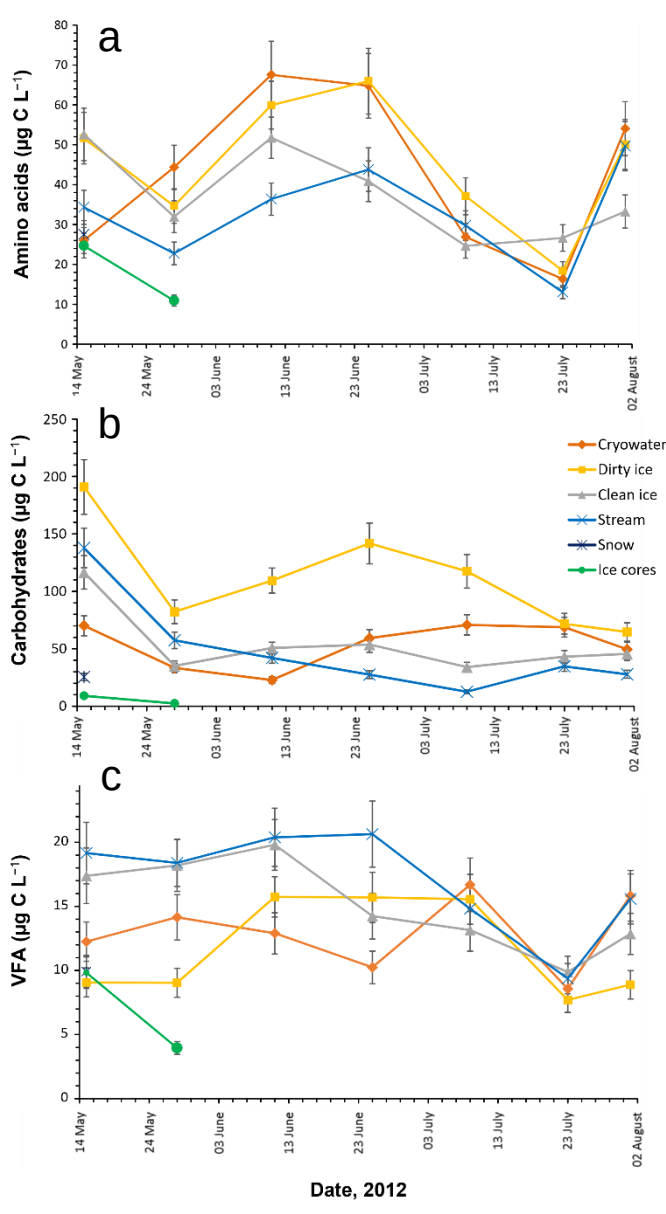
a
Amino acids (µg C L⁻¹)
b
Carbohydrates (µg C L⁻¹)
c
VFA (µg C L⁻¹)
Cryowater
Dirty ice
Clean ice
Stream
Snow
Ice cores
14 May
24 May
03 June
13 June
23 June
03 July
13 July
23 July
02 August
Date, 2012

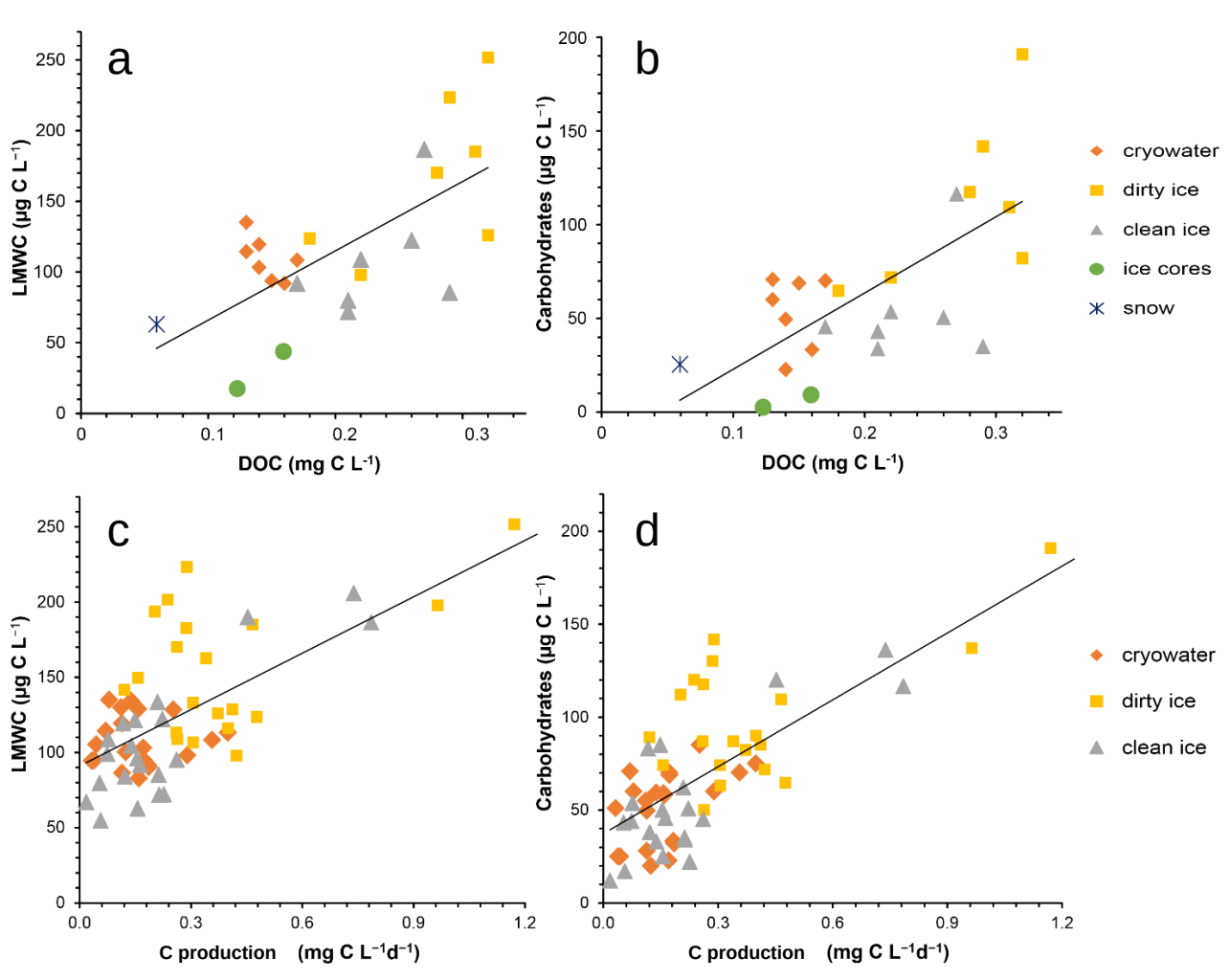
a
b
c
d
LMWC (µg C L⁻¹)
Carbohydrates (µg C L⁻¹)
DOC (mg C L⁻¹)
C production (mg C L⁻¹d⁻¹)
cryowater
dirty ice
clean ice
ice cores
snow